https://doi.org/10.5194/egusphere-2026-1679
Preprint. Discussion started: 10 April 2026

Vicarious calibration of the JAXA Earth Clouds, Aerosols and Radiation Explorer (EarthCARE)/Multi-Spectral Imager (MSI) level 2 cloud product (MSI_CLP) and aerosol product (MSI_ARL)

Minrui Wang[1], Takashi Y. Nakajima[1,2], Jiaqi Wu[2], Yamato Ogura[3], Mayumi Yoshida[3], Masataka Muto[4], Takuji Kubota[4]

[1]Research & Information Center, Tokai University, Kanagawa, 259-1292, Japan
[2]Graduate School of Engineering, Tokai University, Kanagawa, 259-1292, Japan
[3]Remote Sensing Technology Center of Japan, Ibaraki, 305-8505, Japan
[4]Earth Observation Research Center, Japan Aerospace Exploration Agency, Ibaraki, 305-8505, Japan

Correspondence to: Minrui Wang (wang.minrui@tokai.ac.jp)

Abstract. After launch in May 2024, the Earth Clouds, Aerosols and Radiation Explorer (EarthCARE) satellite entered its orbit and commenced operations. In the early studies, it was reported that the initial version of Multi-Spectral Imager (MSI) level 1 data (MSI_RGR) had suffered some issues that compromised the data quality. To solve the issues of the MSI level 1 data, vicarious calibration is necessary particularly for the visible, near infrared, and shortwave infrared (VNS) bands. This paper described the vicarious calibration on MSI_RGR using the geostationary satellite Himawari-9 cloud retrieval as an intermediator. Our results based on the late revised version (vBa) of MSI_RGR verified the data quality improvement work by the ESA MSI level 1 team, which from slight overestimation (calibration coefficient of about 0.93) for the visible band and almost no overestimation or underestimation for near-infrared band in the case of cloud product. On the other side, for aerosol product, slight overestimation (calibration coefficient of about 0.92-0.93) for the visible band and slight underestimation (calibration coefficient of about 1.04-1.07) for near-infrared band. The calibration coefficients derived here will be used for further development of EarthCARE MSI products.

1 Introduction

The assessment of radiative forcing of clouds and aerosols is a major uncertainty in climate change projections with climate models (Masson-Delmotte et al., 2021). The Earth Clouds, Aerosols and Radiation Explorer (EarthCARE), which launched in May 2024, is a joint Earth observation satellite project between the European Space Agency (ESA) and Japan Aerospace Exploration Agency (JAXA) for observing cloud–aerosol interactions (Illingworth et al., 2015). EarthCARE is equipped with four sensors, namely, Cloud Profiling Radar (CPR), Atmospheric Lidar (ATLID), Multi-Spectral Imager (MSI), and Broadband Radiometer (BBR). Data products related to clouds, aerosols, and radiation flux are created from single and combined observations from these sensors (Wehr et al. 2023, Eisinger et al. 2024).

https://doi.org/10.5194/egusphere-2026-1679
Preprint. Discussion started: 10 April 2026

The MSI (Albiñana et al., 2010) has been developed by the ESA and measures emitted infrared and reflected solar radiances. An algorithm of JAXA EarthCARE MSI level 2 cloud product (MSI_CLP) has been developed in Tokai University as described in Wang et al (2023). ~~Besides, an algorithm of~~ JAXA EarthCARE MSI lever 2 aerosol product (MSI_ARL) has been developed as described in Yoshida et al (2021), which was based on the algorithm described in Yoshida et al (2018). MSI_CLP is a part of JAXA L2 Standard Products, while MSI_ARL is a part of JAXA L2 Research Products. The official version vBa of MSI_CLP and MSI_ARL was released in March 2025, and the further update version vCa was released in November 2025. During the early ground-based calibration and initial in-orbit validation phase, it was reported that the initial version of MSI level 1 data (MSI_RGR) suffered from problems that compromised the data quality. ESA (2025) reported that the radiation of the MSI visible, near infrared, and shortwave infrared (VNS) bands (bands 1 to 4) was systematically about 10 % higher than those of the Spinning Enhanced Visible and Infrared Imager (SEVIRI) and Flexible Combined Imager (FCI) (ESA, 2025). The reflectance was 3 % higher in the visible (VIS) band (band 1), and 10 % higher in the 1.6 μm channel (band 3). The ESA and JAXA MSI teams concluded during the workshop that the diffuser (ground) characterization could not be trusted and that vicarious calibration was necessary, particularly for VNS bands (ESA, 2025). With comparisons of the Geostationary Satellite Himawari operated by Japan Meteorological Agency, Muto et al. (2025) indicates that the over-trend of MSI cloud optical thickness (COT) derived from too bright reflectance of visible and near infrared bands. In addition to the onboard calibration, vicarious calibration has been used in previous works (e.g., Murakami et al., 2005; Murakami et al., 2022). The utilization of vicarious calibration can be needed to solve the issues of the MSI level 1 data.

This paper describes a scientific method of vicarious calibration using the Himawari-9 satellite cloud product, which used the same algorithm as MSI_CLP for retrieving cloud properties. By using the Himawari-9 cloud product as an intermediator, we calculated the calibration coefficient of the MSI L1 radiance data for late revised version (vBa).

Section 2 describes the MSI_CLP product, MSI_ARL product, and Himawari-9 cloud product ~~used in this study~~, as well as the methods with which we obtain the calibration coefficient for both MSI_CLP and MSI_ARL. Section 3 presents the results and discussion, and in Sect. 4 we give the conclusions of this study.

2 Sensors, data, and methods

2.1 EarthCARE/MSI

Detailed information about EarthCARE/MSI can be found in our previous work (Wang et al., 2023). After the launch of EarthCARE in May 2024, during the early phase of data processing and validation ~~works,~~ there were problems in the initial version of MSI_RGR, which caused a non-negligible negative effect on the quality of both MSI_RGR and Level 2 products such as the MSI_CLP. Although many of these products have been modified in later updates, as of March 2025, the MSI VNS bands were still overestimated compared with SEVIRI (particularly, 17 % for the VIS band) and FCI (10 % for the VIS band). However, the thermal infrared (TIR) bands agreed well with SEVIRI and FCI (ESA, 2025). Nevertheless, uncertainties, such

https://doi.org/10.5194/egusphere-2026-1679
Preprint. Discussion started: 10 April 2026

as solar irradiance variations in MSI_RGR, directly lead to non-negligible effects on Level 2 cloud and aerosol products because the solar irradiance is used to calculate spectral top of atmosphere (TOA) reflectance as

$$\rho_\lambda = \frac{L_\lambda \pi}{I_{\lambda,c} \cos(\theta_0)} \quad (1)$$

where $I_{\lambda,c}$ is the spectral solar irradiance for each band and MSI across-track pixel, L_λ is the spectral radiance (pixel values for bands 1 to 4 in MSI_RGR) on MSI along- and across-track grid, and θ_0 is the solar zenith angle.

2.2 MSI_CLP

MSI_CLP includes clear confidence level and cloud phase, which are produced by the Cloud and Aerosol Unbiased Decision Intellectual Algorithm (CLAUDIA) (Ishida and Nakajima, 2009), as well as cloud optical thickness (COT), cloud particle effective radius (CER), cloud top temperature (CTT), and cloud top height produced by the Comprehensive Analysis Program for Cloud Optical Measurement (CAPCOM) (Nakajima and Nakajima, 1995; Kawamoto et al., 2001). For detailed information about CLAUDIA and CAPCOM, please refer to our previous work (Wang et al., 2023).

The radiances of the VIS band (band 1) and short-wave infrared (SWIR) band (bands 3 and 4) from MSI L1 data were expected to be significantly overestimated. Therefore, the COT, which is sensitive to the VIS band radiance, and the CER, which is sensitive to the SWIR band radiance, were also expected to be overestimated, which could compromise the data quality.

MSI_CLP uses MSI L1C data as input. The version vBa of MSI_RGR released on 27 May 2025 by ESA, which is a major patch for solving known issues, was used in this study to evaluate the data quality improvement.

We chose two frames from the Frame E data (01807E, 01808E), which are from the oceanic areas around the western Pacific Ocean, and one frame from the Frame D data (01808D), which are from the Japanese coastal ocean area. All data were chosen from 22 September 2024, which is the autumnal equinox on which high solar elevation results in similar scattering angles.

2.3 MSI_ARL

The synergistic exploitation of imaging sensors onboard both geostationary and polar-orbiting satellites provides essential complementary information for characterizing aerosol distributions on a global scale. To advance this objective, Yoshida et al. (2018) developed a unified retrieval algorithm capable of deriving atmospheric aerosol properties across multiple satellite sensors and over diverse surface types, including both land and ocean. In addition, Yoshida et al. (2021) incorporated aerosol transport model forecasts as a priori estimate of retrieval to further enhance the retrieval accuracy.

These methodologies were applied to EarthCARE/MSI channels 1–4. By employing forecast estimation from the Himawari-9/AHI aerosol assimilation system as a priori estimate of retrieval, observations from the geostationary Himawari-9 sensor can effectively inform and support retrievals for the polar-orbiting MSI instrument. This approach facilitates genuine sensor synergy between geostationary and polar-orbiting satellite platforms.

https://doi.org/10.5194/egusphere-2026-1679
Preprint. Discussion started: 10 April 2026

Moreover, the unified algorithm is tailored to each MSI pixel—particularly regarding gas absorption correction, look-up table construction, and surface reflectance treatment—because the MSI Level-1 data exhibit spectral response function variations across the scan, commonly referred to as the "smile effect."

Finally, MSI_ARL includes aerosol optical thickness (AOT) (both ocean and land), as well as Angstrom Exponent (AE) (ocean only), as a part of JAXA MSI L2 research product.

2.4 Himawari-9 cloud product

Himawari-9 is a meteorological geostationary satellite that was launched in November 2016 and is now operated by the Japan Meteorological Agency (JMA). Himawari-9 uses the onboard Advanced Himawari Imager (AHI) to observe the whole of East and Southeast Asia and the western Pacific Ocean with a full disk scan every 10 min. Many of the wavelength bands of AHI are like those of EarthCARE/MSI, including horizontal resolutions of 500 m for VIS (0.65 μm), 1 km for NIR (0.86 μm), and 2 km for SWIR (1.6 and 2.2 μm) and TIR (8.6, 10.4, and 12.4 μm). The JAXA Himawari-9 cloud product uses the same cloud phase algorithm (CLAUDIA) and cloud property algorithm (CAPCOM) as MSI_CLP and thus is suitable for validating MSI_CLP. However, we only used the Himawari-9 cloud product as an intermediator to obtain the cloud properties for the radiative transfer simulation. The radiance data measured by AHI are calibrated by using the onboard calibrators and the framework of the Global Space-based Inter-Calibration System (GSICS) (Takahashi and Okuyama, 2017).

For the objective meteorological data for CAPCOM, we used JRA-3Q long-term reanalysis data provided by JMA, and the minimum surface albedo data calculated from Moderate Resolution Imaging Spectroradiometer (MODIS) channel 1 in October 2017 were also used for CAPCOM retrieval.

We only chose warm water cloud pixels (CTT > 260 K) by screening the data and considered these to be plane-parallel. From the screened Himawari-9 cloud product data, pixels that matched the MSI frames were extracted, and the COT and CER were used as input data for radiative transfer simulation. The lookup table (LUT) we used for Himawari retrieval was only available for 0.65 and 2.2 μm channels (equivalent to MSI bands 1 and 4). Thus, in future work, we need an additional LUT to obtain the calibration coefficient for MSI band 3.

2.5 Concept of the vicarious calibration for MSI_CLP

Figure 1 shows the basic concept of the vicarious calibration and the procedure for our method.

https://doi.org/10.5194/egusphere-2026-1679
Preprint. Discussion started: 10 April 2026

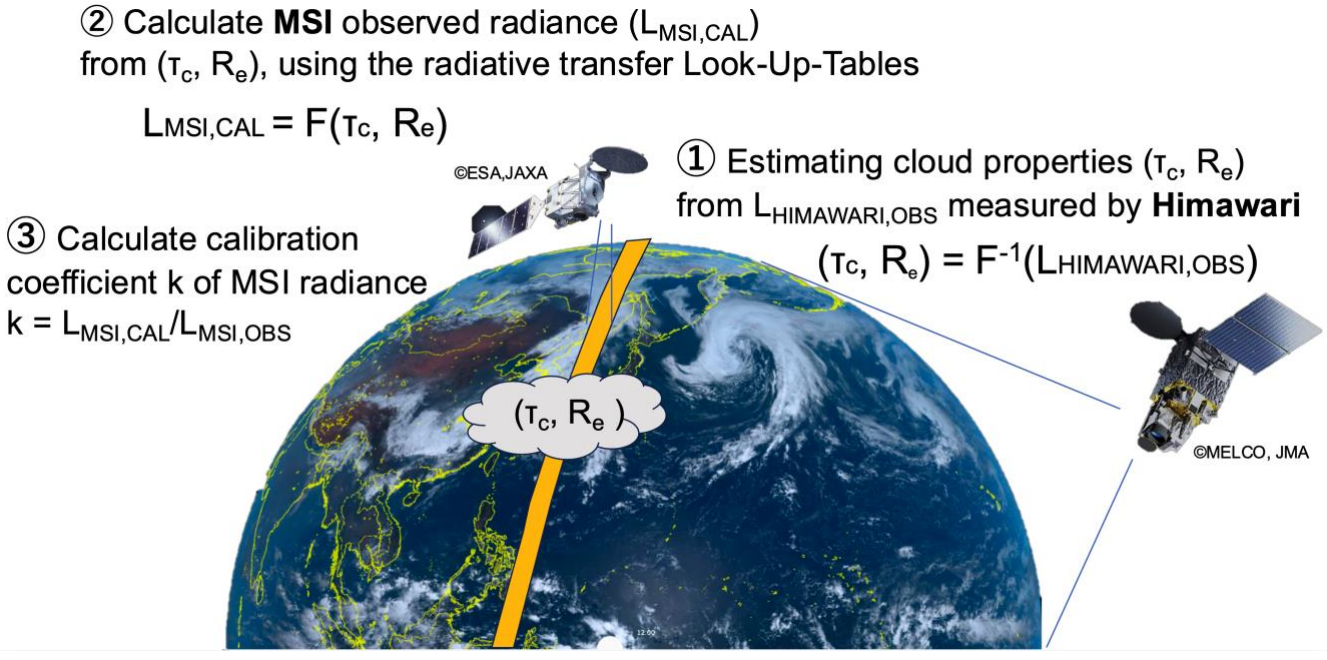

Figure 1: Schematic of the vicarious calibration for MSI_CLP.

Figure 2 shows the flowchart of the vicarious calibration for MSI_CLP.

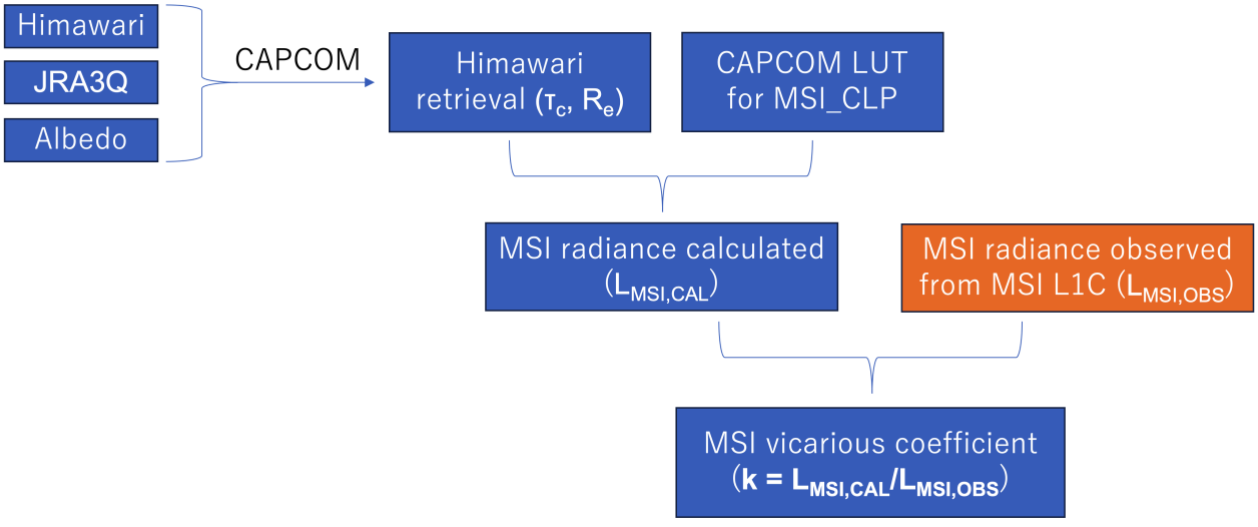

Figure 2: Flowchart of MSI_CLP vicarious calibration.

https://doi.org/10.5194/egusphere-2026-1679
Preprint. Discussion started: 10 April 2026

We chose some typical scenes for water clouds, and estimated cloud properties (COT and CER) from the Himawari-9 cloud product as

$$(\tau_c, R_e) = F^{-1}\left(L_{\mathrm{HIMAWARI,OBS}}\right) \quad (2)$$

where τ_c is COT, R_e is CER, and F^{-1} , the inverse function of F, infers the CAPCOM algorithm, which is used in the Himawari-9 cloud product.

With the COT and CER from Himawari-9 cloud product, we performed a radiative transfer simulation using the CAPCOM LUT for EarthCARE/MSI to calculate the corresponding radiance of MSI as

$$L_{MSI,CAL} = F(\tau_c, R_e) \quad (3)$$

where $L_{\mathrm{MSI,CAL}}$ is the MSI radiance based on the COT and CER obtained from Himawari-9, and F infers the CAPCOM LUT. CAPCOM's cloud property algorithm LUT is grid data that use cloud top altitude as altitude information, which can be considered as a function of COT and CER as

$$F(\tau_c, R_e) \quad (4)$$

Normally, in the CAPCOM algorithm, COT and CER are retrieved from the observed radiance in the MSI L1C data using the inverse function F^{-1} of the LUT. However, in the present method, COT and CER retrieved from Himawari were used as input, and the corresponding radiance ($L_{\mathrm{MSI,\,CAL}}$) was estimated by a radiative transfer calculation.

Finally, we compared the radiance values from the actual MSI L1C data and the estimated values by calculating

$$k = \frac{L_{MSI,CAL}}{L_{MSI,OBS}} \quad (5)$$

where k is the vicarious calibration coefficient of the MSI radiance and $L_{\mathrm{MSI,OBS}}$ is the actual pixel value obtained from the MSI L1C data ~~(which supposed to have overestimation).~~ These data were normalized to obtain the statistical scatter plots, and k was calculated from the average values of $L_{\mathrm{MSI,\,CAL}}$ and $L_{\mathrm{MSI,OBS}}$.

The advantage of this method is that we target clouds observed simultaneously by both EarthCARE/MSI and Himawari-9, which use the same algorithms to obtain the products. Therefore, the cloud physical properties, such as COT and CER, do not depend on which satellite is measuring them or on the solar zenith angle, satellite zenith angle, relative azimuth angles, and wavelengths (response functions) of the observing sensors. The light scattering properties of warm water clouds composed of spherical cloud particles are described well by Mie scattering theory (Mie, 1908), and thus these properties provide an intermediator between Himawari-9 and EarthCARE/MSI cloud products. Our method has also been used in Japan to calibrate previous satellites, such as Advanced Earth Observing Satellite 2 (ADEOS-II) and Global Change Observation Mission for Climate (GCOM-C) (Murakami et al., 2005, 2022). Another method of vicarious calibration based on the ground surface has used high-surface-reflectance data, such as that from deserts. However, desert surfaces have complex scattering characteristics and lack a well-established theory like Mie scattering theory and thus are prone to uncertainty. Furthermore, ground surface calibration involves long distances between the surface and the satellite, requiring large atmospheric corrections that also introduce uncertainty. In contrast, vicarious calibration using water clouds allows Mie scattering theory's characteristics to be used, and the atmospheric correction required between the cloud top and the satellite is small.

https://doi.org/10.5194/egusphere-2026-1679
Preprint. Discussion started: 10 April 2026

2.6 Vicarious calibration for MSI_ARL

We evaluate the MSI L1c observed TOA reflectance at clear sky for the aerosol retrieval. Figure 3 depicts an overview of the methodology for the vicarious calibration. The MSI TOA reflectance is simulated by radiative transfer code called the System for the Transfer of Atmospheric Radiation, whose development was initially led by the University of Tokyo (STAR, Nakajima and Tanaka 1986, 1988; Stamnes et al., 1988) by using the corresponding Himawari-9 Level-2 aerosol products of AOT, AE, and Single Scattering Albedo (SSA). Because the Himawari-9 aerosol retrieval algorithm is same as that of MSI (Yoshida et al. 2018,2021), the MSI simulated TOA reflectance can be estimated consistently with the Himawari-9 observations. Finally, the simulated TOA reflectance is compared with the observed MSI L1c TOA reflectance for the vicarious calibration.

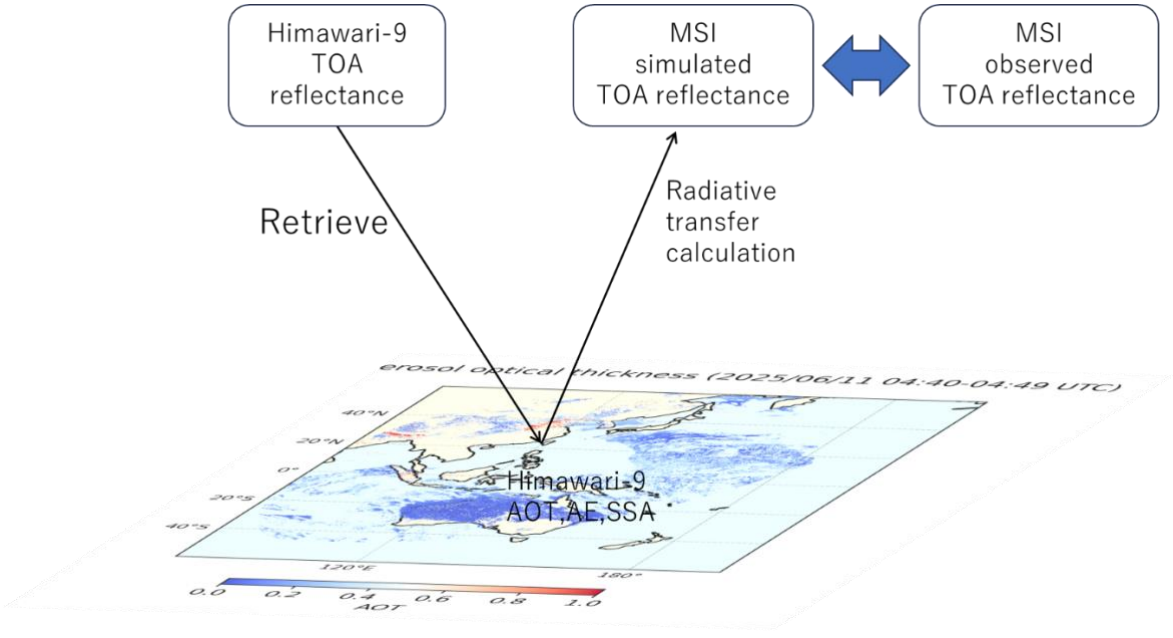

Figure 3: Overview of the methodology for the vicarious calibration for aerosol retrieval.

MSI L1c data version vBa from April 1, 2025 to July 14, 2025 is used for the vicarious calibration. The area we use for the calibration is the clear sky pixels over ocean without sun-glint within 5 pixels around, where wind speed is less than 5 m/s. For the quality check on satellite data, we use the spatially uniform MSI data within 5 pixels whose sensor zenith angle is less than 30 degrees. In addition, we used the only good quality Himawari aerosol data whose AOT is less than 0.2 to minimize the impact on the simulated TOA reflectance from the retrieval errors in Himawari aerosol products.

https://doi.org/10.5194/egusphere-2026-1679
Preprint. Discussion started: 10 April 2026

3 Results and discussion

3.1 Result of MSI_CLP

3.1.1 Data use of MSI_CLP

Figures 4 and 5 show the distribution of COT and CER using the 2.21 μm channel from the 01807E and 01808E frames of MSI_CLP. EarthCARE/MSI takes about 12 min to finish a single frame, whereas the time gap between two Himawari-9 cloud products is 10 min. To ensure that the most accurate reference objects were selected, we identified water cloud pixels from MSI_CLP as target objects and obtained their observation times. We selected the closest corresponding pixels with the observation time from Himawari-9 cloud products as source data for retrieving COT and CER. For frame E across the equator, we selected water cloud pixels with latitudes no higher than 10 °N or 10 °S as our objects. We also selected frame 01808D as a reference to determine whether there were significant differences between the results from the mid-latitude coastal areas of Japan and those near the equator.

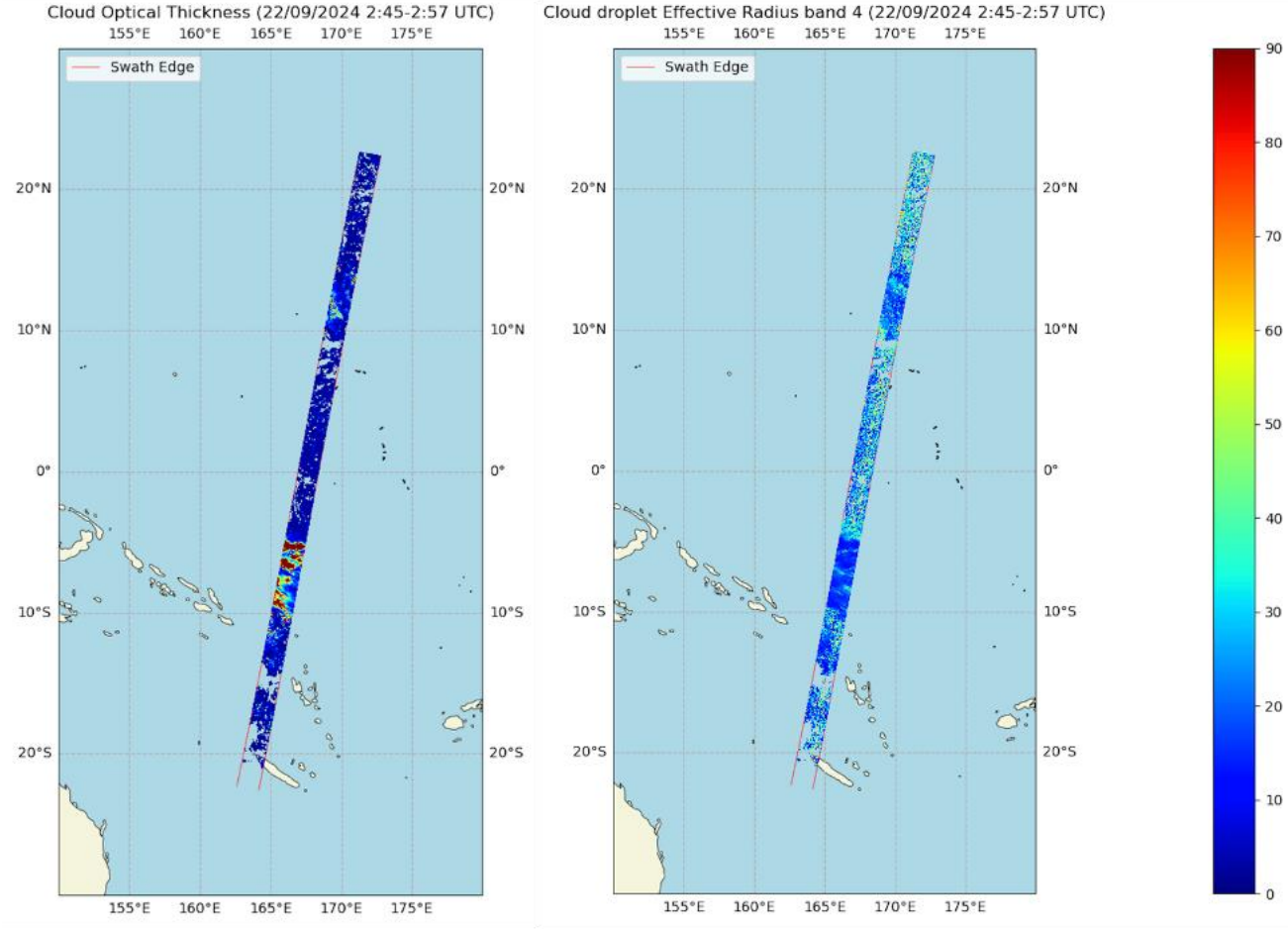

https://doi.org/10.5194/egusphere-2026-1679
Preprint. Discussion started: 10 April 2026

Figure 4: Cloud properties (left: COT, right: CER using 2.21 μm) from MSI_CLP frame 01807E (2:45–2:57 UTC on 22 September 2024).

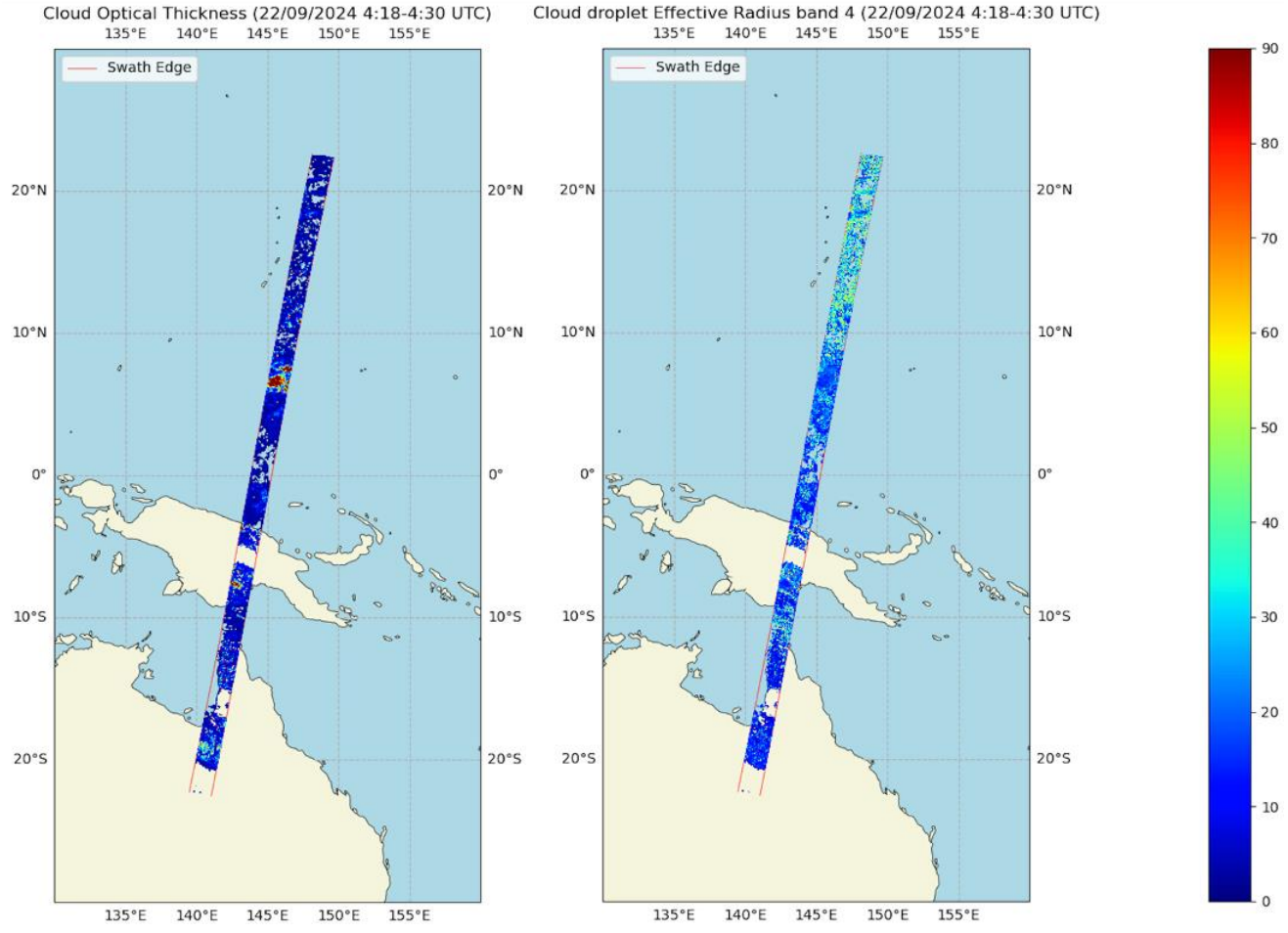

Figure 5: Cloud properties (left: COT, right: CER using 2.21 μm) from MSI_CLP frame 01808E (4:18–4:30 UTC on 22 September 2024).

3.1.2 Himawari-9 cloud product

Figures 6–8 show the Himawari-9 cloud product (COT and CER using 2.21 μm) that matched the time of our three chosen frames. For frame 01807E and 01808E, typical oceanic scenes for the western Pacific Ocean were measured with widespread cloud cover. From the products matched with 01807E, 01808D, and 01808E, 54,861, 62,367, and 77,471 pixels were screened, respectively. The northern red area in the product matched with 01808D was a fill value area because the solar zenith angle

https://doi.org/10.5194/egusphere-2026-1679
Preprint. Discussion started: 10 April 2026

maximum limitation of CAPCOM for Himawari-9 was exceeded. Because the cloud areas of Himawari-9 and MSI that matched were around 40 °N, the fill value area at 50 to 60 °N did not negatively affect our work. Some cloud pixels in Himawari-9 and MSI's tracks matched but were above land or islands, and these pixels were excluded from follow-up procedures.

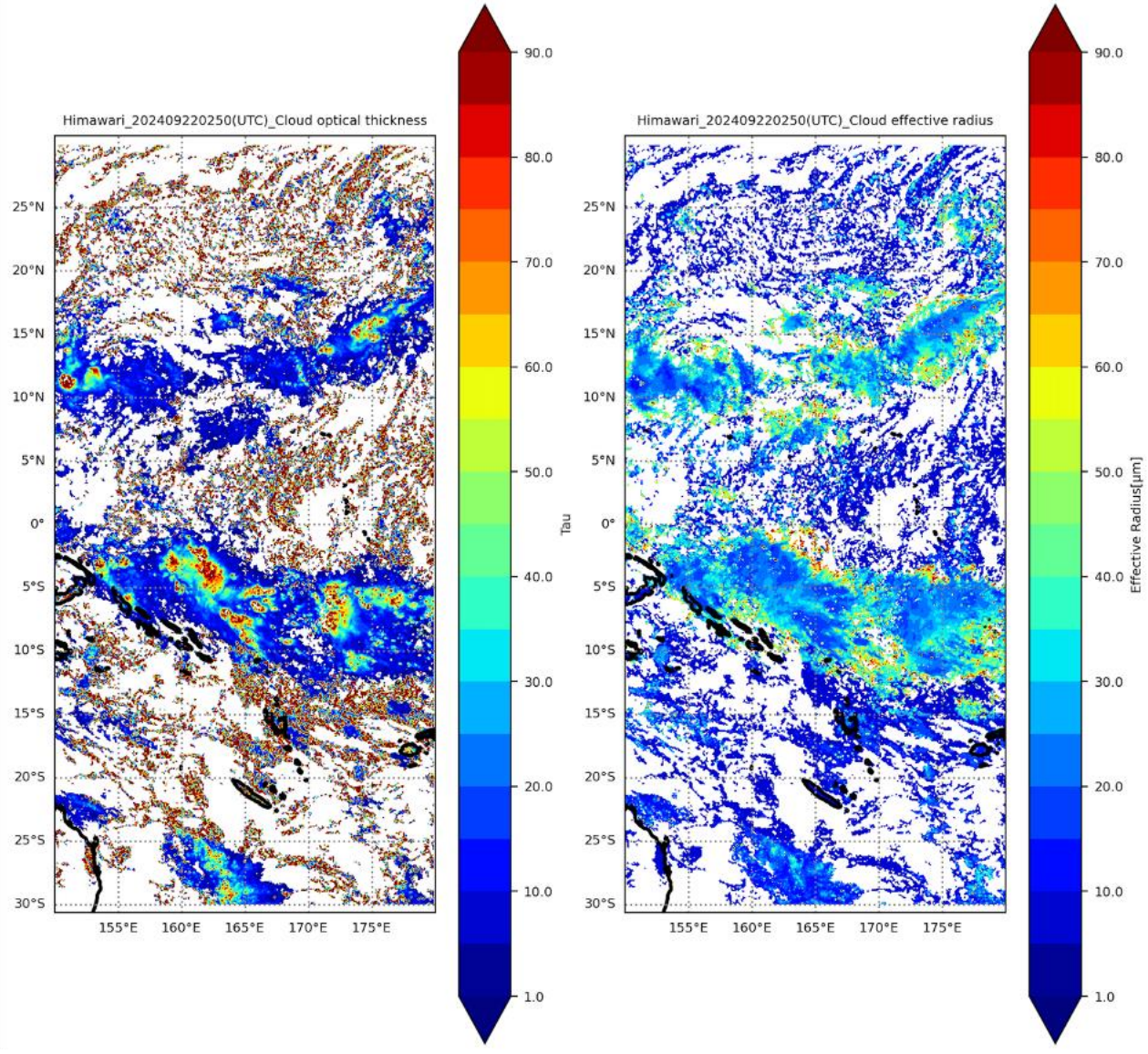

Figure 6: Himawari-9 cloud products (left: COT, right: CER using 2.21 μm) that matched the time of MSI_CLP frame 01807E.

https://doi.org/10.5194/egusphere-2026-1679
Preprint. Discussion started: 10 April 2026

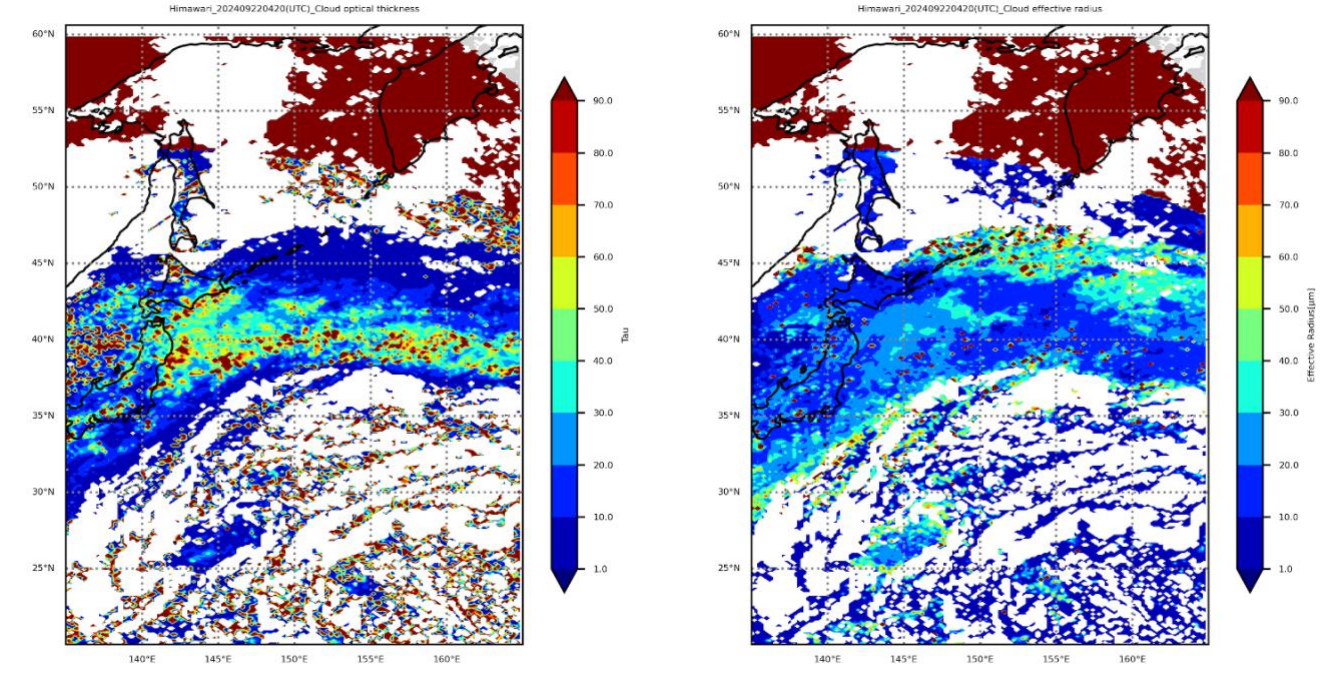

215 **Figure 7: Himawari-9 cloud products (left: COT, right: CER using 2.21 μm) that matched the time of MSI_CLP frame 01808D.**

https://doi.org/10.5194/egusphere-2026-1679
Preprint. Discussion started: 10 April 2026

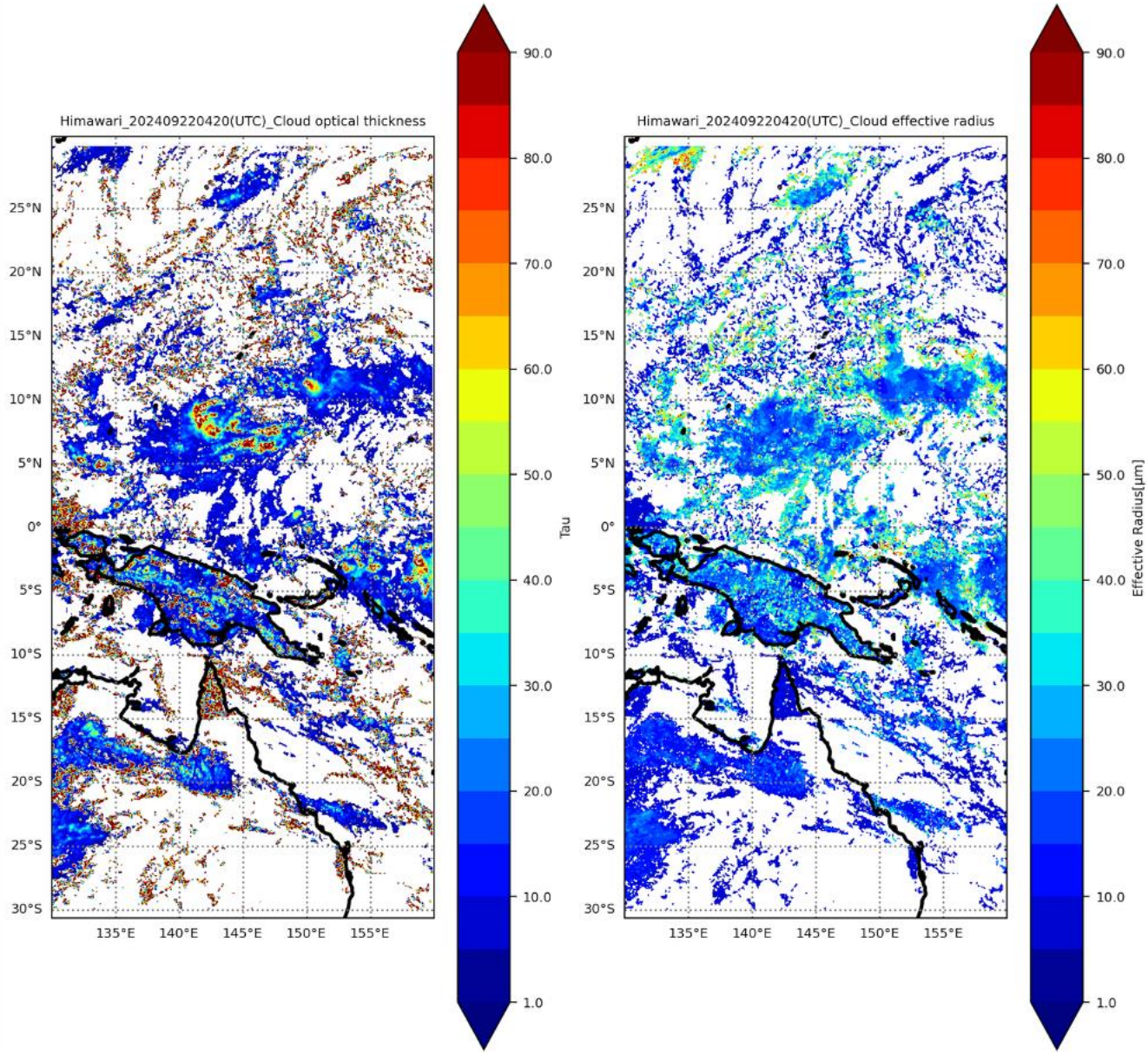

Figure 8: Himawari-9 cloud products (left: COT, right: CER using 2.21 μm) that matched the time of MSI_CLP frame 01808E.

3.1.3 Calibration coefficient for MSI_CLP

The vBa results of the calibration coefficient are listed and discussed.

Figures 9–11 show the statistical scatter plots of normalized $L_{MSI,OBS}$ and $L_{MSI,CAL}$ for MSI frames 01807E, 01808E, and 01808D, respectively, with the revised version (vBa) of MSI_RGR. The calibration coefficients for band 1 were 0.93, 0.94,

https://doi.org/10.5194/egusphere-2026-1679
Preprint. Discussion started: 10 April 2026

and 0.92 for frames 01807E, 01808E, and 01808D, respectively, indicating that there was still overestimation in MSI_RGR (vBa) VIS radiation. In contrast, for band 4, all three frames produced consistent results showing that the radiance of 2.21 µm closely matched the calculated value obtained by Himawari-9 cloud retrieval, with two of the three frames even showing a slight underestimation trend. This result has delighted both us and the ESA team because it indicates that the series of fixes implemented in the MSI_RGR vBa version have yielded major improvements, at least in the SWIR channels.

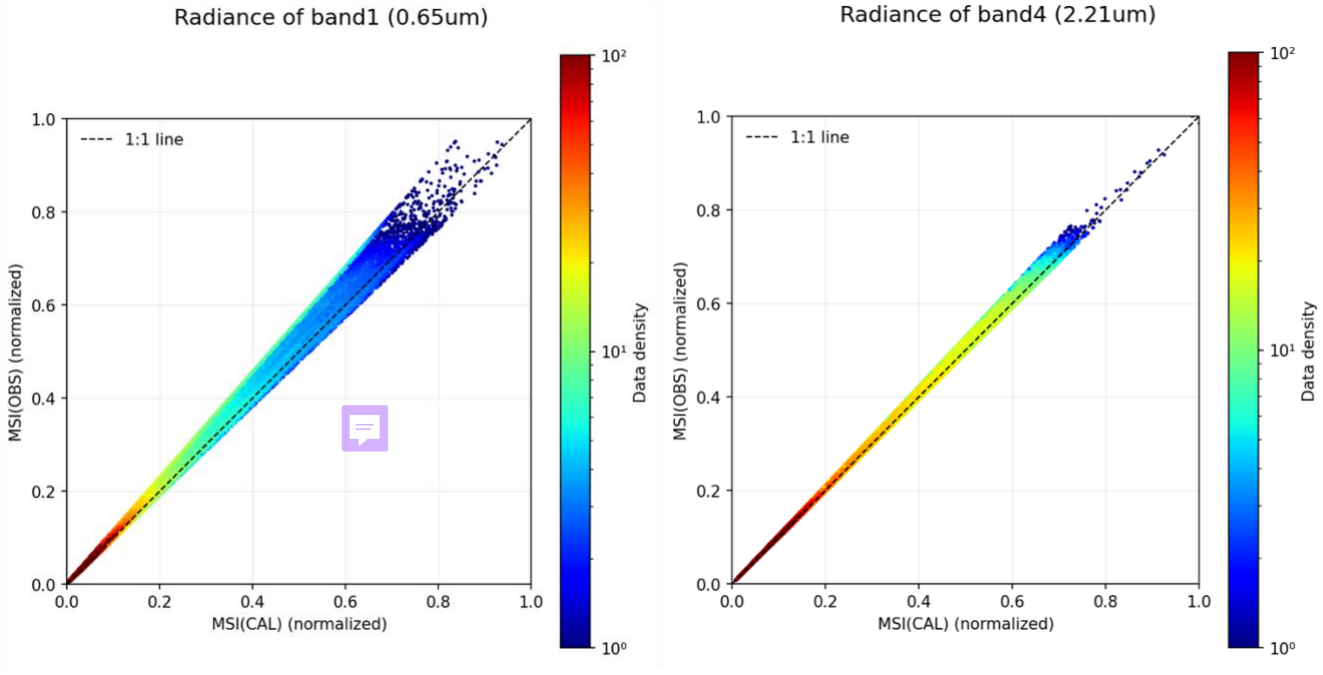

Figure 9: Statistical scatter plots of normalized $L_{MSI,OBS}$ and $L_{MSI,CAL}$ for MSI frame 01807E (left: band 1 (0.65 µm), right: band 4 (2.21 µm)) of revised version (vBa). The total number of screened water cloud pixels is 54,861. The vicarious calibration coefficient is 0.93 for band 1, and 0.99 for band 4.

https://doi.org/10.5194/egusphere-2026-1679
Preprint. Discussion started: 10 April 2026

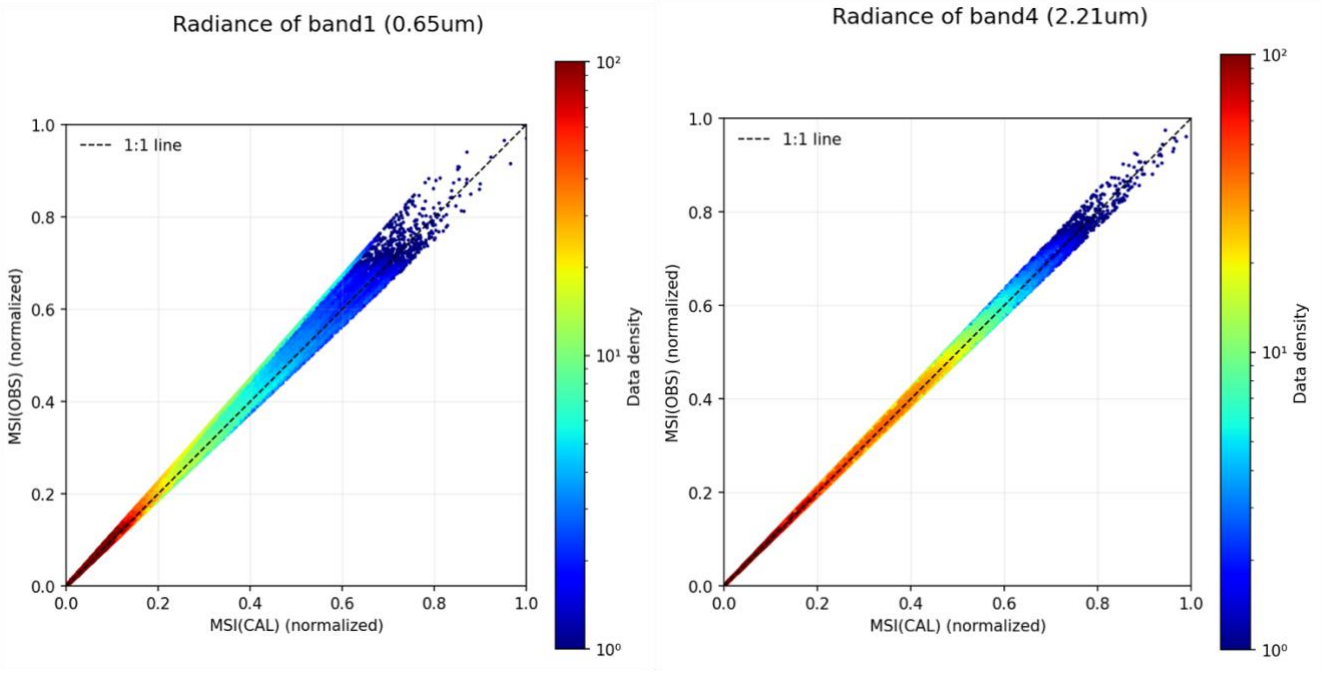

Figure 10: Statistical scatter plots of normalized $L_{MSI,OBS}$ and $L_{MSI,CAL}$ for MSI frame 01808E (left: band 1 (0.65 µm), right: band 4 (2.21 µm)) of revised version (vBa). The total number of screened water cloud pixels is 77,471. The vicarious calibration coefficient is 0.94 for band 1 and 1.02 for band 4.

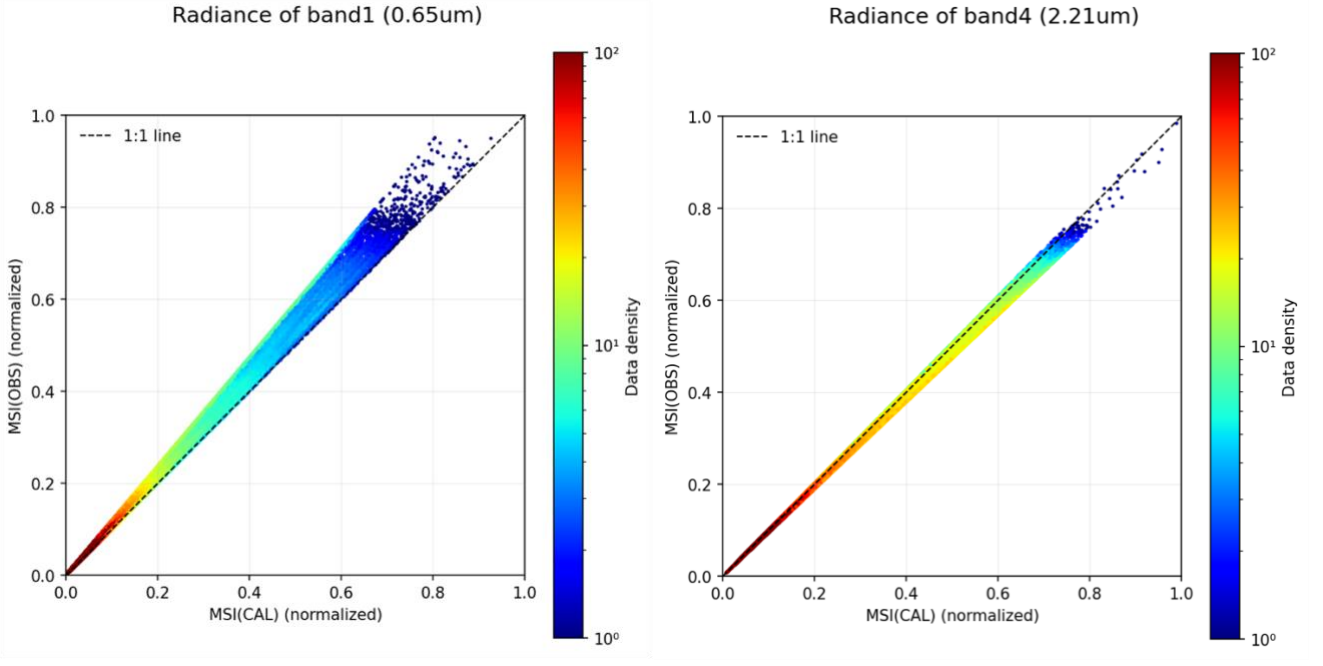

https://doi.org/10.5194/egusphere-2026-1679
Preprint. Discussion started: 10 April 2026

Figure 11: Statistical scatter plots of normalized $L_{MSI,OBS}$ and $L_{MSI,CAL}$ for MSI frame 01808D (left: band 1 (0.65 µm), right: band 4 (2.21 µm)) of revised version (vBa). The total number of screened water cloud pixels is 62,367. The vicarious calibration coefficient is 0.92 for band 1 and 1.04 for band 4.

3.2 Result of MSI_ARL

The example of original MSI L1c observed TOA radiance are shown in Figure 12. Figure 13 depicts the Himawari-9 AOT, AE, and SSA products that match the time of MSI observation shown in Fig.12. Note that the Himawari-9 aerosol products use the same retrieval algorithm (Yoshida et al., 2018 and 2021) as that of MSI_ARL. The MSI TOA reflectance is simulated by using these Himawari-9 aerosol product. For the simulation we use the MSI aerosol Look Up Tables (LUTs) for MSI_ARL calculated by using radiative transfer code STAR.

The examples of the quality-checked observed TOA reflectance used for the vicarious calibration are displayed in Fig. 14 left panel. It validates that the clear and less noisy pixels over ocean are appropriately used for the calibration. We also show the simulated TOA reflectance in the same area in Fig.14 right panel. By comparing these reflectances, we confirmed that the MSI simulated reflectance are generally consistent with the MSI observed reflectance.

Finally, the Figure 15 shows the frequency distributions of the MSI observed and simulated TOA reflectance. The calculated vicarious calibration coefficients are 0.934, 0.920, 1.076, and 1.048 at band 1, 2, 3, and band 4., respectively. We confirmed from the calibrations that the MSI L1c vBa observed reflectance is overestimated in band 1 and 2, but underestimated in band 3 and 4 at the lower reflectance.

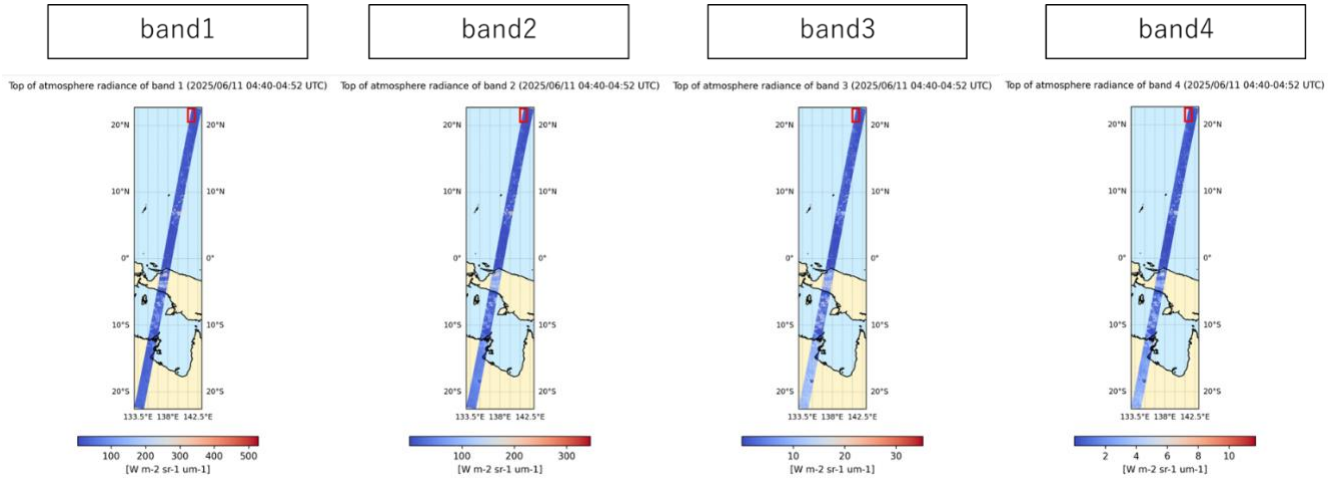

Figure 12: MSI L1c ver. vBa TOA radiance observed at 04:40-04:52 UTC on 11 June 2025.

https://doi.org/10.5194/egusphere-2026-1679
Preprint. Discussion started: 10 April 2026

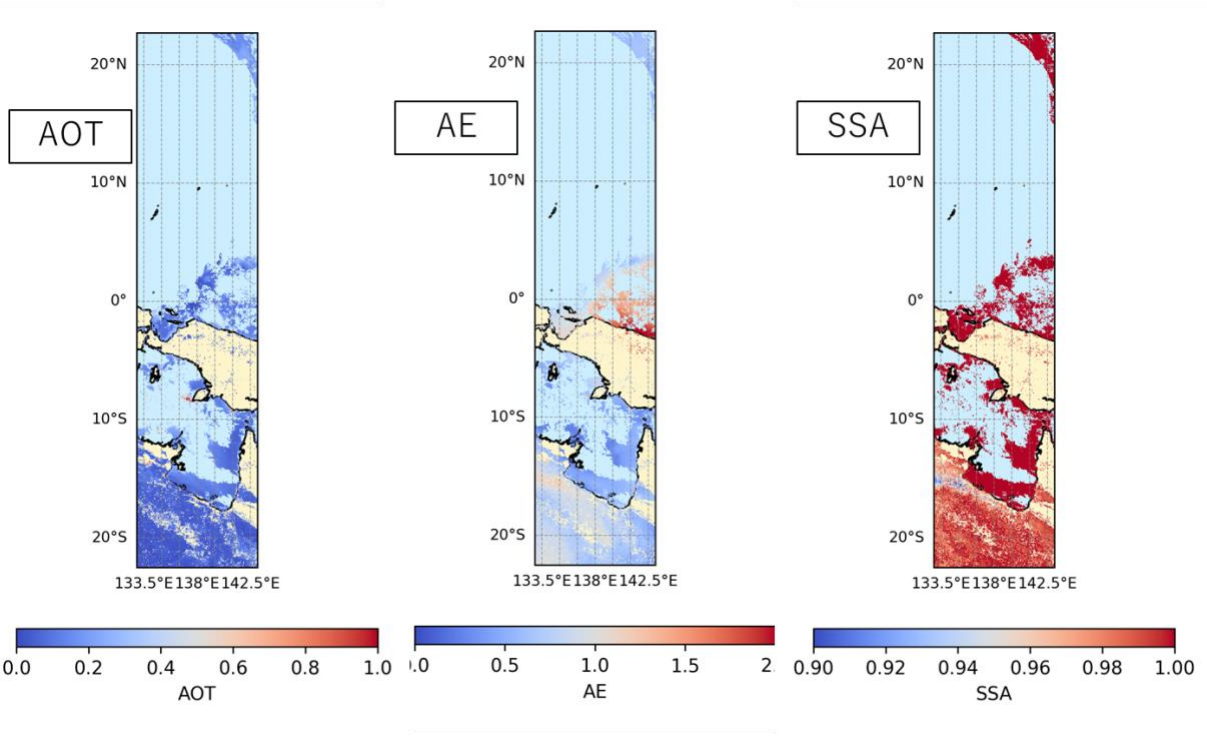

Figure 13: Himawari-9 AOT (left), AE (center), and SSA (right) that matched the time of MSI observation shown in Fig.12.

https://doi.org/10.5194/egusphere-2026-1679
Preprint. Discussion started: 10 April 2026

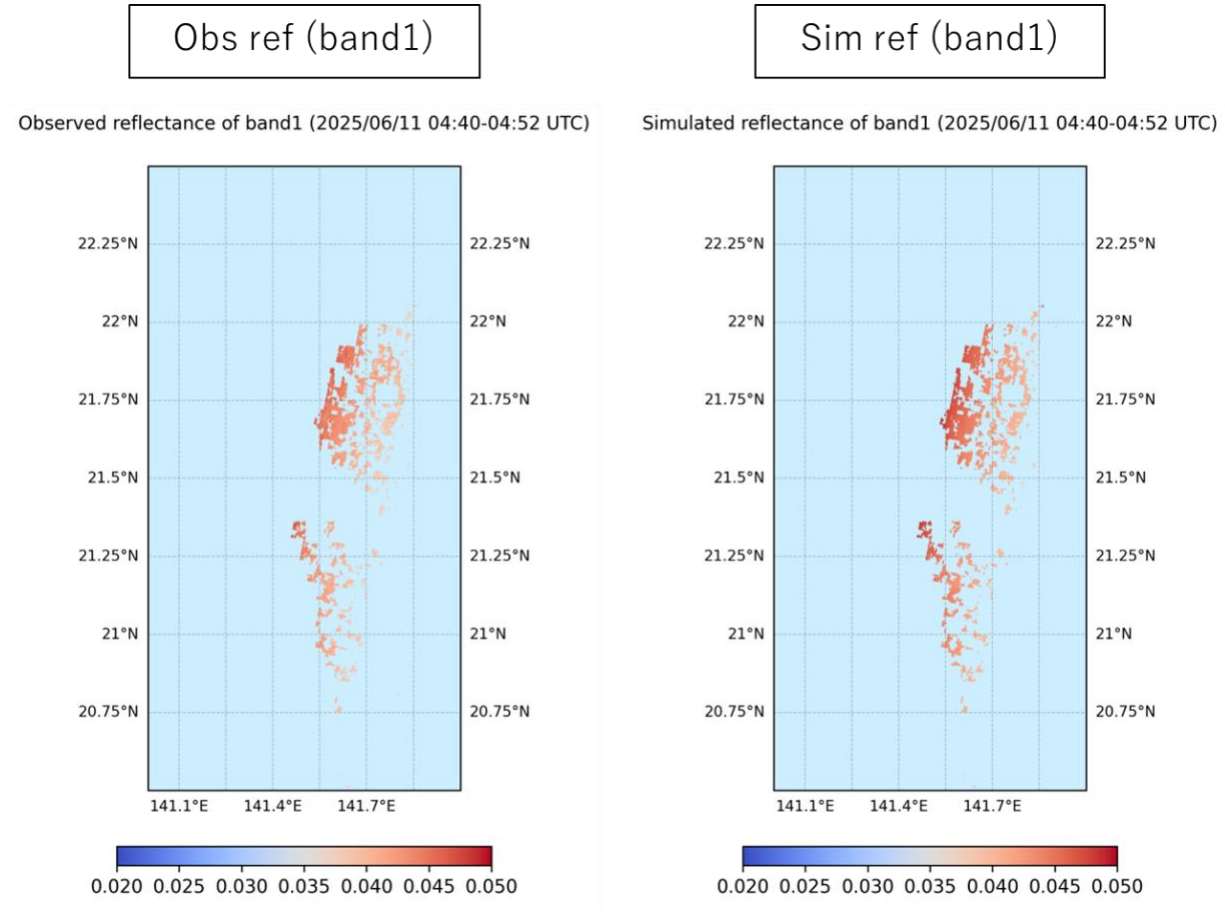

Figure 14: MSI observed (left) and simulated (right) TOA reflectance at band1 used for the vicarious calibration on 11 June 2025 in the red square area in Fig.12.

https://doi.org/10.5194/egusphere-2026-1679
Preprint. Discussion started: 10 April 2026

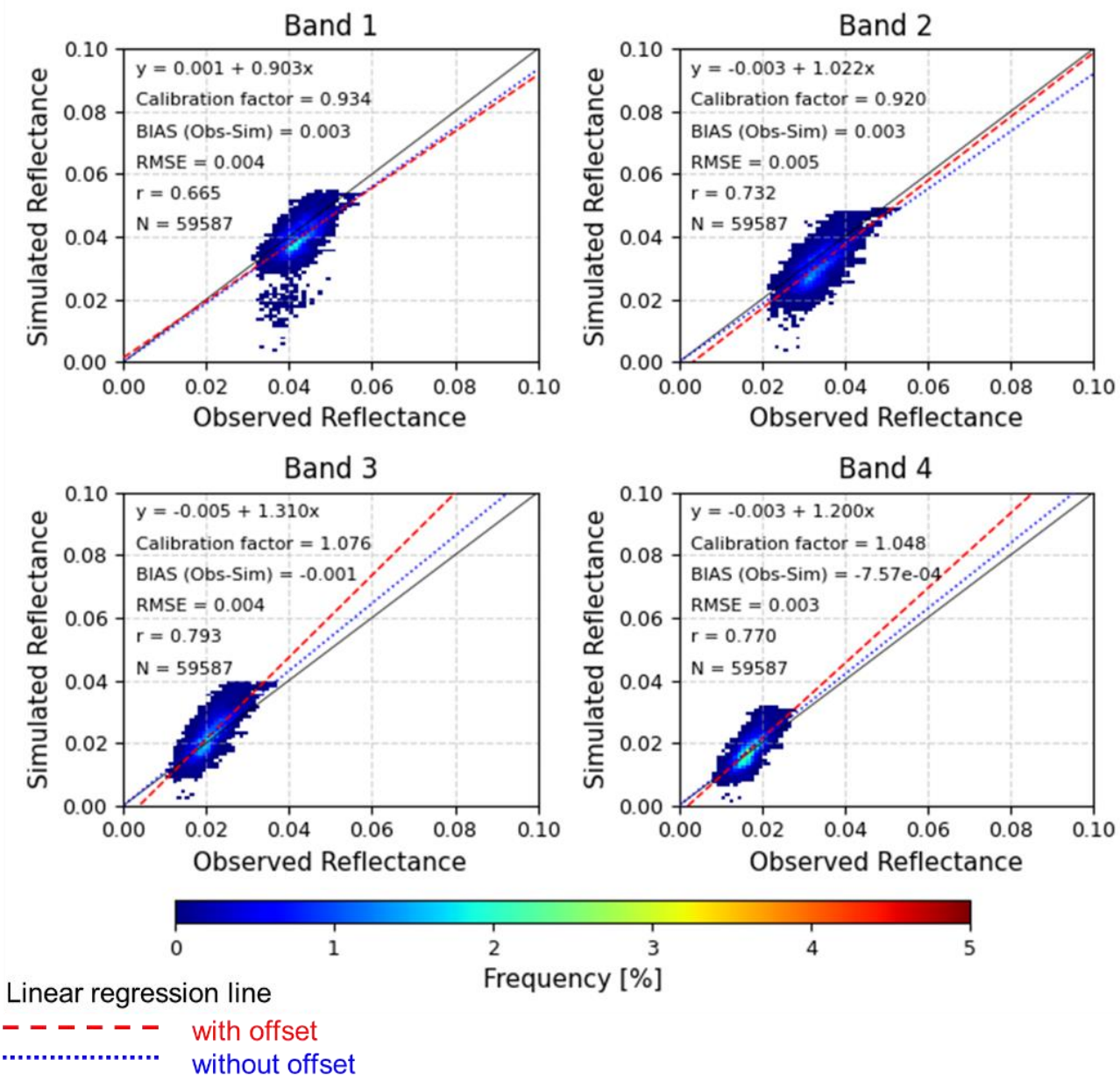

Figure 15: Frequency distribution of observed and simulated reflectance at MSI band1, 2, 3, and 4, and linear regression line with offset (red) and without offset (blue).

275

https://doi.org/10.5194/egusphere-2026-1679
Preprint. Discussion started: 10 April 2026

4 Conclusions

In this study, two MSI frames with a high concentration of water clouds were carefully selected from the equatorial ocean area on the autumnal equinox, along with one MSI frame selected from the mid-latitude coastal area of Japan. Himawari-9 cloud products were used to retrieve COT and CER, and the MSI water cloud LUT was read to perform radiative transfer calculations, which were then used to calculate vicarious calibration coefficients for MSI bands 1 (VIS band) and 4 (NIR band).

For MSI_CLP (vBa), the VNS overestimation was mitigated compared with early version, but COT was still overestimated, and the calibration coefficient for band 1 was around 0.92–0.94. In contrast, CER showed no significant overestimation or underestimation, and the calibration coefficient for band 4 was 0.99–1.04, indicating that nearly no calibration is needed.

For MSI_ARL (vBa), still slight overestimation (calibration coefficient of about 0.92-0.93) was confirmed for the visible band (band 1 and band 2), and for near-infrared band (band 3 and band 4), slight underestimation (calibration coefficient of about 1.04-1.07) was confirmed.

The calibration coefficient obtained from this study was applied to the further update version vCa while reading MSI_RGR, and validation by JAXA was operated in autumn 2025 to ensure that our calibration completes the work properly.

Code and data availability

The source code used in this study is not publicly available because of restrictions related to proprietary algorithms. However, the MSI_CLP and MSI_ARL product data are now publicly available from the JAXA G-Portal (https://gportal.jaxa.jp/gpr/information/product#EarthCARE).

Author contributions

TYN designed the basic framework of calibrations, and MW carried them out. TYN developed and provided the base model of CAPCOM, which was adapted for this study by MW. JW operated the Himawari-9 cloud retrievals for the vicarious calibration. Gracious advice and assistance were provided from TK and MM during the overall study. JW prepared the manuscript with contributions from all co-authors.

Competing interests

The authors declare that they have no conflict of interest.

Financial support

No funding was received for this study.

https://doi.org/10.5194/egusphere-2026-1679
Preprint. Discussion started: 10 April 2026

References

Albiñana, A. P. Gelsthorpe, R., Lefebvre, A., Sauer, M., Weih, E., Kruse, K.-W., Münzenmayer, R., Baister, G., and Chang, M. T.: The multi-spectral imager on board the EarthCARE spacecraft, in: Proceedings of the Infrared Remote Sensing and Instrumentation XVIII (Proc. SPIE 7808), San Diego, CA, 1–5 August 2010, 780–815, https://doi.org/10.1117/12.858864, 2010.

ESA: 2nd ESA-JAXA EarthCARE in-orbit validation workshop report, ESA-EOPG-EOPGMQ-RP-2025-4, https://airdrive.eventsair.com/eventsairwesteuprod/production-nikal-public/fb0210d1861f4a0e9ae7773c6646717c (last access: 20 March 2025), 2025.

Illingworth, A., Barker, H., Beljaars, A., Ceccaldi, M., Chepfer, H., Delanoe, J., Domenech, C., Donovan, D., Fukuda, S., Hirakata, M., Hogan, R., Huenerbein, A., Kollias, P., Kubota, T., Nakajima, T., Nakajima, T., Nishizawa, T., Ohno, Y., and Okamoto, H.: The EARTHCARE satellite: the next step forward in global measurements of clouds, aerosols, precipitation and radiation, B. Am. Meteorol. Soc., 96, 1311–1332, https://doi.org/10.1175/BAMS-D-12-00227.1, 2015.

Ishida, H. and Nakajima, T. Y.: Development of an unbiased cloud detection algorithm for a spaceborne multispectral imager, J. Geophys. Res., 114, D07206, https://doi.org/10.1029/2008JD010710, 2009.

Kawamoto, K., Nakajima, T., and Nakajima, T. Y.: A global determination of cloud microphysics with AVHRR remote sensing, J. Climate, 14, 2054–2068, https://doi.org/10.1175/15200442(2001)014<2054:AGDOCM>2.0.CO;2, 2001.

Kikuchi, M., Oki, R., Kubota, T., Yoshida, M., Hagihara, Y., Takahashi, C., Ohno, Y., Nishizawa, T., Nakajima, T. Y., Suzuki, K., Satoh, M., Okamoto, H., and Tomita, E.: Overview of Earth, Clouds, Aerosols and Radiation Explorer (EarthCARE) – integrative observation of cloud and aerosol and their radiative effects on the climate system –, J. Remote Sens. Soc. Jpn., 39, 181–196, https://doi.org/10.11440/rssj.39.181, 2019 (in Japanese).

Masson-Delmotte, V., Zhai, P., Pirani, A., Connors, S. L., Péan, C., Berger, S., Caud, N., Chen, Y., Goldfarb, L., Gomis, M. I., Huang, M., Leitzell, K., Lonnoy, E., Matthews, J. B. R., Maycock, T. K., Waterfield, T., Yelekçi, O., Yu, R., and Zhou, B. (Eds.): Climate Change 2021: The Physical Science Basis. Contribution of Working Group I to the Sixth Assessment Report of the Intergovernmental Panel on Climate Change, Cambridge University Press, Cambridge, UK and New York, NY, 2391 pp., 2021.

Mie, G.: Contributions to the optics of turbid media, particularly of colloidal metal solutions, Ann. Phy., 25, 377–445, https://doi.org/10.1002/andp.19083300302, 1908.

Murakami, H., Yoshida, M., Tanaka, K., Fukushima H., Toratani, M., Tanaka A., and Senga, Y.: Vicarious calibration of ADEOS-2 GLI visible to shortwave infrared bands using global datasets, IEEE Trans. Geosci. Remote Sens., 43, 1571–1584, https://doi.org/10.1109/TGRS.2005.848425, 2005.

Murakami, H., Antoine, D., Vellucci, V., and Frouin, R.: System vicarious calibration of GCOM-C/SGLI visible and near-infrared channels, J. Oceanogr., 78, 245–261, https://doi.org/10.1007/s10872-022-00632-x, 2022.

https://doi.org/10.5194/egusphere-2026-1679
Preprint. Discussion started: 10 April 2026

Nakajima, T., and Tanaka, M.: Matrix formulation for the transfer of solar radiation in a plane-parallel scattering atmosphere. J. Quant. Spectrosc. Radiat Transfer, 35, 13–21, 1986.

Nakajima, T., and Tanaka, M.: Algorithms for radiative intensity calculations in moderately thick atmospheres using a truncation approximation. J. Quant. Spectrosc. Radiat. Transfer, 40, 51–69, 1988.

Nakajima, T. Y. and Nakajima, T.: Wide-area determination of cloud microphysical properties from NOAA AVHRR measurements for FIRE and ASTEX regions, J. Atmos. Sci., 52, 4043–4059, https://doi.org/10.1175/15200469(1995)052<4043:WADOCM>2.0.CO;2, 1995.

Stamnes, K., Tsay, S. C., Wiscombe, W., and Jayaweera, K.: Numerically stable algorithm for discrete-ordinate-method radiative transfer in multiple scattering and emitting layered media. Appl. Opt., 27, 2502–2509, 1988.

Takahashi M. and Okuyama S.: Introduction to the Global Space-based Inter-Calibration System (GSICS) and calibration/validation of the Himawari-8/AHI visible and infrared bands, Meteorol. Sat. Cent. Tech. Note, 62, 1–18, 2017 (in Japanese).

Wang, M., Nakajima, T. Y., Roh, W., Satoh, M., Suzuki, K., Kubota, T., and Yoshida, M.: Evaluation of the spectral misalignment on the Earth Clouds, Aerosols and Radiation Explorer/multi-spectral imager cloud product, Atmos. Meas. Tech., 16, 603–623, https://doi.org/10.5194/amt-16-603-2023, 2023.

Yoshida, M, Kikuchi, M., Nagao, T. M., Murakami, H., Nomaki, T., and Higurashi, A.: Common retrieval of aerosol properties for imaging satellite sensors, J. Meteor. Soc. Japan, https://doi.org/10.2151/jmsj.2018-039, 2018.

Yoshida, M., Yumimoto, K., Nagao, T. M., Tanaka, T., Kikuchi, M., and Murakami, H.: Retrieval of Aerosol Combined with Assimilated Forecast, Atmos. Chem. Phys., 21, 1797, https://doi.org/10.5194/acp-21-1797-2021, 2021.